JACS
JOURNAL OF THE AMERICAN CHEMICAL SOCIETY
Article
pubs.acs.org/JACS

WMe_6 Tamed by Silica: $\equiv Si-O-WMe_5$ as an Efficient, Well-Defined Species for Alkane Metathesis, Leading to the Observation of a Supported W–Methyl/Methylidyne Species

Manoja K. Samantaray,[†] Emmanuel Callens,*[,†] Edy Abou-Hamad,[†] Aaron J. Rossini,[‡] Cory M. Widdifield,[‡] Raju Dey,[†] Lyndon Emsley,[‡] and Jean-Marie Basset*[,†]

[†]KAUST Catalysis Center (KCC), King Abdullah University of Science & Technology, 23955-6900 Thuwal, Saudi Arabia

[‡]Institut de Sciences Analytiques (CNRS, ENS-Lyon, UCB Lyon 1), Université de Lyon, Centre de RMN à Très Hauts Champs, 5 rue de la Doua, 69100 Villeurbanne, France

Supporting Information

ABSTRACT: The synthesis and full characterization of a well-defined silica-supported $\equiv Si-O-W(Me)_5$ species is reported. Under an inert atmosphere, it is a stable material at moderate temperature, whereas the homoleptic parent complex decomposes above −20 °C, demonstrating the stabilizing effect of immobilization of the molecular complex. Above 70 °C the grafted complex converts into the two methylidyne surface complexes $[(\equiv SiO-)W(\equiv CH)Me_2]$ and $[(\equiv SiO-)_2W(\equiv CH)Me]$. All of these silica-supported complexes are active precursors for propane metathesis reactions.

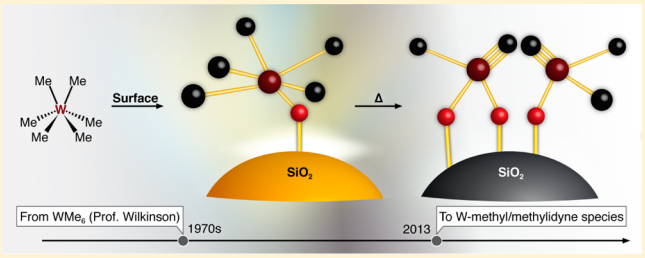

INTRODUCTION

Transformation of linear alkanes into their lower and higher homologues via alkane metathesis is an important process in the petrochemical industry.[1] To date, two main families of catalytic systems exist for alkane metathesis: (i) a dual-catalyst system which relies on a dehydrogenation/hydrogenation catalyst combined with an olefin metathesis catalyst[2,3] and (ii) a "multifunctional" single-site catalyst supported on various oxides which is able to achieve these three reactions.[4,5] Since the first disclosed silica-supported tantalum hydride,[5] we have reported various single-site supported catalysts for alkane metathesis employing Ta and W polyhydrides directly linked to silica, silica–alumina, and alumina.[4,6,7] These catalysts have been successfully synthesized and characterized at the molecular and atomic level. Most of them were found to transform light alkanes into their lower and higher homologues.[6,8] In these instances, the first step of C–H bond activation occurred on the metal hydride, and the resulting alkyl species were assumed to undergo either a process of α- or β-H elimination to give the corresponding carbene or olefin, both of which are key intermediates for the olefin metathesis process.[9] Although the most active catalysts are generated from surface metal hydrides, supported catalysts which contain a neopentyl/neopentylidene moiety were also found to be slightly active in alkane metathesis.[8] It was therefore assumed that an alkyl/hydride functional group is needed to provide an alkylidene to convert alkene intermediates via a metallacyclobutane.[10,11]

It is well-known that W/Ta alkylidene complexes discovered by Wilkinson[12] and later Schrock[13] are key active catalysts in olefin metathesis, which is one of the various steps occurring in single-site alkane metathesis. Thus, the preparation of such species as single sites on surfaces together with alkyl/hydride moieties is of high interest for alkane metathesis. However, in the past, several approaches to synthesize surface methylidene species have been used with little success.[14,15] Here we envisage that a polymethyl tungsten complex possessing no β-H would be a suitable alternative candidate to the neopentyl ligand to generate an *in situ* surface W–methylidene species in its highest oxidation state.

Given that the most active supported catalysts for single-site alkane metathesis are d^0 $W^{(VI)}$ complexes,[6] we propose to immobilize a well-defined homoleptic hexamethyltungsten complex to assess if its transformation into a W–methylidene would affect the catalytic performance of this alkane metathesis process.

Here we use WMe_6, (**1**), initially discovered by Wilkinson, as the precursor in this strategy.[12] We report the preparation and characterization, at the molecular level, of a well-defined supported $\equiv Si-O-W(Me)_5$ (**2**) (Scheme 1), its activity toward alkane metathesis, and the isolation of a novel silica-supported W–methyl/methylidyne species.

Received: October 23, 2013
Published: December 26, 2013

dx.doi.org/10.1021/ja410747g | J. Am. Chem. Soc. 2014, 136, 1054–1061

Scheme 1. Synthesis of Supported ≡Si−O−W(Me)$_5$ (2) by Reaction of 1 with Partially Dehydroxylated Silica

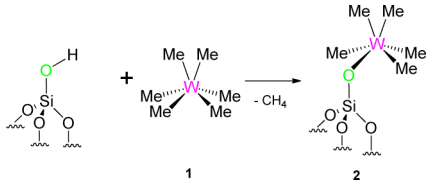

RESULTS AND DISCUSSION

Preparation and Characterization of ≡Si−O−W(Me)$_5$ on SiO$_{2\text{-}700}$. Grafting of **1** on silica has already been reported by Whan,[16,17] though the system, in 1972, was poorly characterized by today's standards. In the following we re-examine this step using the appropriate analytical tools of modern surface organometallic chemistry (e.g., solid-state NMR, IR, and elemental analysis).[18]

A modified synthetic protocol was employed for the synthesis of **1**.[19] With freshly sublimed WCl_6 in CH_2Cl_2 as the starting material, 3 equiv of Me_2Zn yielded the desired complex **1** (12% yield). Solution NMR spectroscopy experiments (^{1}H, ^{13}C, and ^{1}H−^{13}C HSQC) on the product in CD_2Cl_2 are consistent with the formation of **1** and also agree with previously reported spectroscopic data (see the Supporting Information).[19] Next, the grafting of **1** was realized by stirring a mixture of an excess of **1** and silica which had been partially dehydroxylated at 700 °C (i.e., SiO$_{2\text{-}700}$, which contains 0.3 ± 0.1 mmol of silanol groups/g) at −50 °C under an inert atmosphere of argon. After several washing cycles with pentane and drying under high vacuum, the resulting yellow powder **2** contains 3.5−3.9 wt % tungsten and 1.1−1.3 wt % carbon as determined by elemental analysis (C/W ratio 5.0 ± 0.1, in comparison to the expected value of 5).

An IR spectrum of **2** showed decreased intensity of the bands at 3742 cm^{-1}, which are associated with isolated and geminal silanols. For **2**, two new groups of bands in the 3014−2878 and 1410 cm^{-1} regions were observed. These are assigned to ν(CH) and δ(CH) vibrations of the methyl ligands bonded to tungsten (see the Supporting Information). Hydrogenolysis of **2** at 150 °C produced 5 equiv of CH_4 per W atom. Mass balancing and gas quantification are consistent with **2** being assigned to ≡Si−O−W(Me)$_5$.

Further spectroscopic analyses of **2** were also conducted with solid-state NMR. The ^{1}H magic-angle spinning (MAS) solid-state NMR spectrum of **2** displays one signal at 2.0 ppm (Figure 1A) which autocorrelates in double-quantum (DQ) and triple-quantum (TQ) NMR experiments under 22 kHz MAS as shown in Figure 1B,C, respectively.[20] This strong autocorrelation peak is attributed to the methyl groups (2.0 ppm chemical shift in the single-quantum frequency; 4.0 and 6.0 ppm in indirect dimensions of the DQ and TQ spectra, respectively). The ^{13}C CP/MAS NMR spectrum shows a single peak at 82 ppm (Figure 1D). This carbon resonance correlates with the protons at a chemical shift of 2.0 ppm, as indicated in the 2D ^{1}H−^{13}C HETCOR NMR spectrum recorded with a contact time of 0.2 ms (Figure 1E). The ^{1}H and ^{13}C chemical shifts are similar to those observed in the solution NMR spectra of molecular **1**. Note that grafting of **1** on oxide supports could result in the formation of monopodal or bipodal grafted species due to strained silica ring defects produced after thermal dehydroxylation.[21] ^{1}H and ^{13}C solid-state NMR spectroscopy of a ^{13}C-enriched sample of **2** (95% ^{13}C labeled) did not indicate the presence of a signal at or near 0 ppm (in both spectra), which would indicate methyl transfer to an adjacent silicon atom of silica and hence the formation of the bipodal species [(≡Si−O)$_2$W(Me)$_4$][≡Si-Me] (see Figure S6 in the Supporting Information for an analogous example).

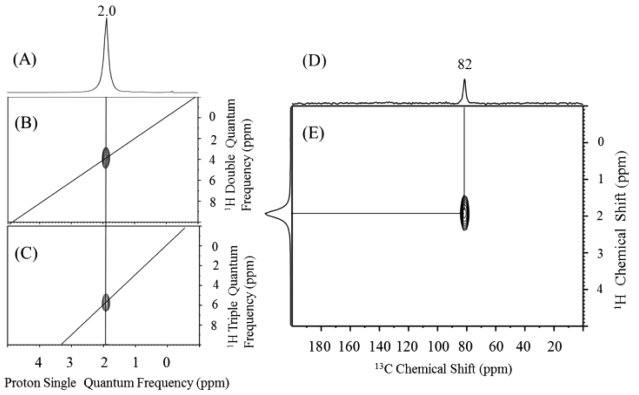

Figure 1. (A) One-dimensional (1D) ^{1}H MAS solid-state NMR spectrum of **2** acquired at 600 MHz (14.1 T) with a 22 kHz MAS frequency, a repetition delay of 5 s, and 8 scans. (B) Two-dimensional (2D) ^{1}H−^{1}H double-quantum (DQ)/single-quantum (SQ) and (C) ^{1}H−^{1}H triple-quantum (TQ)/SQ NMR spectra of **2** (both acquired with 32 scans per t_1 increment, 5 s repetition delay, 32 individual t_1 increments). (D) ^{13}C CP/MAS NMR spectrum of **2** acquired at 9.4 T (ν_0(^{1}H) = 400 MHz) with a 10 kHz MAS frequency, 1000 scans, a 4 s repetition delay, and a 2 ms contact time. An exponential line broadening of 80 Hz was applied prior to Fourier transformation. (E) 2D ^{1}H−^{13}C CP/MAS dipolar HETCOR spectrum of **2** (acquired at 9.4 T with an 8.5 kHz MAS frequency, 2000 scans per t_1 increment, a 4 s repetition delay, 64 individual t_1 increments, and a 0.2 ms contact time). For all spectra depicted here, **2** was 95% ^{13}C labeled.

The anchoring of **1** on partially dehydroxylated silica would substitute a strong σ-donor methyl group with a weaker σ-donor siloxy group. Consequently, we should expect different chemical shifts for W−methyl groups (trans or cis to the W−O−Si≡ fragment). From the ^{1}H and ^{13}C NMR spectra recorded at 298 K, only one signal was observed. We have previously reported that grafted molecular species are highly dynamic, and therefore it is possible that dynamic motion results in the observation of a set of averaged chemical shifts.[22,23] Thus, we recorded the ^{1}H and ^{13}C solid-state NMR spectra of **2** at reduced temperatures.

Figure 2A,B shows the variable-temperature ^{13}C CP/MAS and ^{1}H spin echo MAS solid-state NMR spectra of **2**, which had been isotopically enriched to 95% in ^{13}C. At 301 K, a single resonance is observed at 82.2 and 2.0 ppm in the ^{13}C and ^{1}H NMR spectra, respectively. However, as the temperature of the sample was reduced, the ^{13}C resonance broadened until it splits into two separate resonances centered at 94.2 and 74.1 ppm with a 1.0:1.8 intensity ratio (Figure 2A). The variation in the ^{1}H MAS NMR spectra when the temperature was decreased was similar, and two distinct resonances centered at 2.6 and 1.7 ppm are observed at 196 K. Room-temperature ^{1}H and ^{13}C chemical shifts are observed at the weighted average of the respective low-temperature chemical shifts. Note that the peak appearing at low temperature at −0.5 ppm in the ^{1}H NMR spectra presumably corresponds to residual methane on the surface.

This clearly indicates that the observation of a single resonance at room temperature results from a fast chemical exchange (on the NMR time scale) between the two

dx.doi.org/10.1021/ja410747g | J. Am. Chem. Soc. 2014, 136, 1054−1061

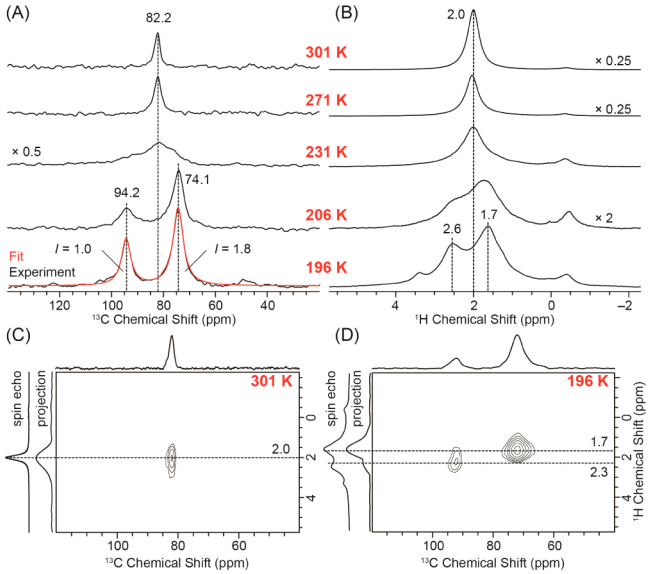

Figure 2. Variable-temperature (A) ^{13}C CP/MAS and (B) ^{1}H spin echo MAS solid-state NMR spectra of **2** with 95% ^{13}C labeling of the methyl groups at 16.4 T. Sample temperatures, isotropic chemical shifts, and intensity scaling factors (which account for differences in the number of scans) are indicated. A fit of the 196 K ^{13}C CP/MAS NMR spectrum is shown (red trace), and the integrated intensities of the two resonances are indicated. Two-dimensional $^{1}H-^{13}C$ dipolar HETCOR NMR spectra of **2** acquired at (C) 301 K with a contact time of 0.75 ms and (D) 196 K with a contact time of 0.25 ms. Both HETCOR spectra were acquired with 16 scans per t_1 increment, 80 individual t_1 increments, and t_1 incremented by 64 μs for each t_1 point. During t_1, *e*-DUMBO-1_{22} homonuclear ^{1}H decoupling was applied and proton chemical shifts were corrected by dividing the apparent ^{1}H chemical shift dimension by a scaling factor of 0.57.[24] The true sample temperatures were calibrated by separately measuring the ^{79}Br isotropic chemical shifts and longitudinal relaxation times of KBr.[25]

nonequivalent types of methyl groups which possess a 2:3 stoichiometry. A low-temperature $^{1}H-^{13}C$ dipolar HETCOR NMR spectrum clearly shows that the less intense high-frequency ^{1}H and ^{13}C resonances correlate (2.6 ppm, 94.2 ppm) while the more intense low-frequency resonances correlate (1.7 ppm, 74.1 ppm) (Figure 2D).

In order to better understand the local structure of the supported species in **2** and to explain the observed variable-temperature NMR data, we performed DFT calculations. Prior to modeling **2**, we validated the computational methods by calculating the structure of molecular **1**, which exhibits sd^5 hybridization at the metal center, as demonstrated with valence bond theory by Landis et al.[26,27] and molecular orbital and *ab-initio* calculations by Eisenstein et al.[28] Additionally, we performed geometry optimizations and NMR chemical shift calculations for several W molecular systems presented earlier by Schrock and co-workers for which high-quality experimental solution NMR data were available.[29,30] Our present DFT calculation predicts that WMe_6 possesses a trigonal-prismatic geometry (i.e., C_{3v} symmetry), which is in reasonable agreement with the W−C bond lengths and C−W−C bond angles of the X-ray structure.[31]

The DFT model of **2** also possesses a similar pseudo-trigonal-prismatic arrangement of the ligands (Figure 3A). Two of the methyl groups (labeled 3 and 5) are directed away from the silica surface, while the other three methyl groups (labeled 1, 2, and 4) are closer to the silica surface. As a consequence of

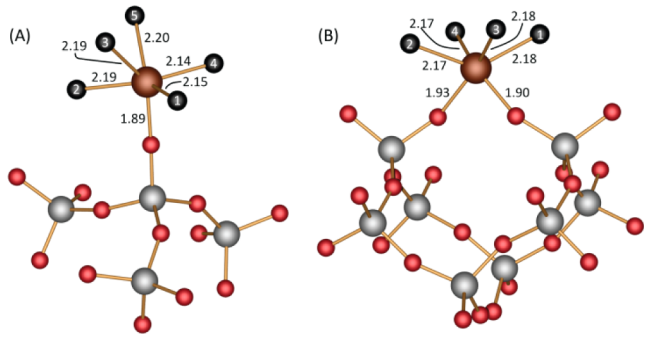

Figure 3. DFT optimized structural model for (A) **2** and (B) selected local environment for the computational model of the bipodal $W(Me)_4$ species in **3**. Tungsten−carbon and tungsten−oxygen internuclear distances are indicated in angstroms. Calculated isotropic ^{1}H and ^{13}C chemical shifts are provided in Table 1. Complete molecular coordinates are specified in Tables S2 and S3 (Supporting Information). For clarity, all hydrogen atoms have been omitted.

these distinct bonding environments, the ^{1}H and ^{13}C chemical shifts for methyl groups 1, 2, 4 and 3, 5 are calculated to differ by 0.82 and 18.4 ppm, respectively (Table 1), which is in very

Table 1. DFT Calculated ^{1}H and ^{13}C Nuclear Magnetic Shieldings and Chemical Shifts for Selected Sites in Models of 2 and the Supported $W(Me)_4$ Species in 3

methyl group	$\sigma_{iso}(^{13}C)$ (ppm)	$\delta_{iso}(^{13}C)$ (ppm)[a]	$\sigma_{iso}(^{1}H)$ (ppm)[b]	$\delta_{iso}(^{1}H)$ (ppm)[a]
		Model System **2**		
1	120.68	–	28.46	–
2	121.89	–	28.98	–
3	99.64	–	27.58	–
4	117.95	–	28.66	–
5	103.41	–	27.41	–
av 1, 2, 4	120.17	60.0	28.70	2.18
av 3, 5	101.52	78.4	27.50	3.00
$\Delta\delta$(3,5−1,2,4)	–	18.4	–	0.82
		Model System $W(Me)_4$ in **3**		
1	108.19	–	27.70	–
2	105.62	–	27.55	–
3	92.98	86.8	27.17	3.23
4	106.64	–	28.47	–
av 1, 2, 4	106.82	73.2	27.91	2.72

[a]The ^{13}C and ^{1}H chemical shifts were obtained by calibrating shielding values with calculations for other molecular tungsten species for which chemical shifts have been previously reported (see the Supporting Information for full details, including the resulting calibration curves). [b]The isotropic shielding values of the three protons of each methyl group have been averaged.

good agreement with the observed shift differences of 0.9 ppm (2.6−1.7 ppm (Figure 2B)) and 20.1 ppm (94.2−74.1 ppm (Figure 2A)) (see the Supporting Information for further computational details). The geometry optimized structural model for the supported species in **2** and the calculated chemical shift differences are consistent with the low-temperature NMR spectra and indicate that two resonances with a 2:3 intensity ratio between high- and low-frequency shifts are expected in both the ^{1}H and ^{13}C NMR spectra. Therefore, the single resonance observed in the room-temperature ^{1}H and ^{13}C NMR spectra are indeed very likely the result of fast exchange

dx.doi.org/10.1021/ja410747g | J. Am. Chem. Soc. 2014, 136, 1054−1061

of the inequivalent methyl groups by rapid rotation (or hopping) about the Si−O−W and different O−W−C bond axes.

Preparation and Characterization of ≡Si−O−W(Me)$_5$ and (≡SiO−)$_2$W(Me)$_4$ on SiO$_{2\text{-}200}$. In addition, we examined the grafting of WMe$_6$ on silica which had been partially dehydroxylated at 200 °C (SiO$_{2\text{-}200}$). Immobilizing an organometallic species on less dehydroxylated silica leads frequently to

Scheme 2. Monopodal and Bipodal Variants of Supported WMe$_6$

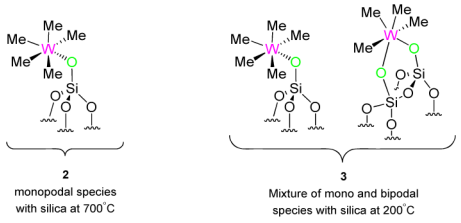

a mixture of monopodal and bipodal species (Scheme 2).[21,32] ^{13}C CP/MAS NMR spectra of **1** supported on silica treated at 200 °C (species **3**) and 700 °C (species **2**) both display similar chemical shifts of the methyl groups attached to the W metal at room temperature. This suggests that we could not distinguish the monopodal species from the bipodal species of **3** at room temperature using ^{1}H/^{13}C solid-state NMR (see Figure S6 in the Supporting Information). Variable-temperature NMR was once again used to identify the structural components of **3**.

At room temperature, a single broad resonance is observed at 80.4 ppm in the ^{13}C CP/MAS spectrum of the product resulting from the grafting of WMe$_6$ on SiO$_{2\text{-}200}$ (**3**). Upon cooling, the single resonance of **3** observed at 298 K splits into two distinct resonances with approximately a 2:3 intensity ratio. However, at 196 K, there is clearly an additional weak "shoulder" visible on the low-frequency peak (Figure S7, Supporting Information). This feature becomes even more pronounced at 150 K. This third resonance is expected to correspond to a bis-grafted tetramethyl species, since it was not observed in any of the NMR spectra of **2**. DFT calculations using a model structure of the bipodal species (≡SiO−)$_2$W(Me)$_4$ were performed to confirm the assignment of the NMR spectrum (Figure 3B).

The DFT model of the bipodal supported species in **3** indicates that three of the carbon nuclei possess magnetic shielding values between 105.6 and 108.2 ppm and are likely shifted to higher frequency relative to the analogous group of three methyl carbons in **2** (average shifts are 73.2 ppm vs 60.0 ppm). The remaining fourth carbon nucleus is predicted to possess a chemical shift that is 13.6 ppm higher than that for the other three methyl groups (86.8 ppm).[33] The additional experimentally observed shift at 75.5 ppm in the 150 K ^{13}C NMR spectrum is therefore assigned to three of the carbons of the bipodal species in **3** (Figure S7, Supporting Information). We then assume that the fourth carbon of the bipodal species in **3** overlaps with the high-frequency shifts of the monopodal species in **3** (which are centered at 91.6 ppm). From a fit of the 150 K ^{13}C CP/MAS NMR spectrum of **3** acquired at 9.4 T, the ratio of the pentamethyl to tetramethyl carbon nuclei was found to be 0.77:0.23 (after subtracting 0.056 from the high-frequency integral to account for overlap with the fourth carbon of the monopodal species). After accounting for the stoichiometry of the methyl groups in the two species, it is possible to derive an overall ratio of around 2.7 pentamethyl species for each tetramethyl species. Therefore, variable-temperature ^{13}C CP/MAS NMR in combination with quantum chemical calculations allowed for the quantification of the surface podality in the systems considered here.

Evaluation of the Apparent Catalytic Activity of 2 and 3 for Propane Metathesis. After the successful synthesis and characterization of complex **2**, we investigated its efficiency as a catalyst precursor for alkane metathesis reactions. Up to now, two supported catalyst systems were found to be able to convert alkanes into higher and lower homologues: (i) supported metal hydrides MH$_x$ (M = Ta, W; x = 1−3) and (ii) supported M(neopentyl)$_x$(alkylidene/alkylidyne) species (M = Ta, W, Mo; x = 1−3).[4]

Although no catalysts containing only sp^3 alkyl ligands have been previously disclosed, we hypothesized that complex **2** would be an excellent candidate for the alkane metathesis reaction. The intuitively easier loss of methane vs neopentane, via the σ-bond metathesis step, potentially offers a significant advantage when using catalyst **2** relative to a neopentyl-containing catalyst.

In our previous work, the propane metathesis reaction was the standard catalytic reaction, and thus to compare the catalytic activity of **2** with earlier results, the catalytic reaction was conducted under the same reaction conditions (a batch reactor, 1 atm of propane, and over a 5 day period at 150 °C).[10] The experimental results confirm our hypothesis of increased catalytic activity for **2** relative to the prior species. Indeed, propane was successfully catalyzed when introducing **2** into the reaction (127 TONs) and appears to compare favorably with the previously reported inactive catalyst ≡Si−O−W(≡CtBu)(CH$_2$$t$Bu)$_2$ or the relatively much less reactive complex ≡Si−O−WH$_x$ (8 TONs).[34] As anticipated, when **3** was used in the reaction vessel, the propane metathesis reaction was less efficient (47 TONs), in support of the notion that the higher functional number of methyl groups on the silica surface provides better activity (see Table 2).

Table 2. Propane Metathesis Reaction: Activity (TON) and Alkane Product Selectivities of W Catalyst Precursors 2 and 3 at 150 °C

		product selectivity (%)[b]			
catalyst precursor	TON (conversion (%))[a]	methane	ethane	butanes[c]	pentanes[d]
≡SiO$_{2\text{-}700}$−W(Me)$_5$	127 (12)	2	54	33/4	6/1
≡SiO$_{2\text{-}200}$−W(Me)$_x$	47 (5)	7	56	22/2.5	9/2

[a]TON is expressed in (mol of propane transformed)/(mol of W). [b]The selectivities are defined as the amount of product over the total amount of products. Ratio of linear and branched alkanes. [c]C$_4$/i-C$_4$. [d]C$_5$/i-C$_5$.

The alkane product distributions when using these two different supported species in the reaction vessel are very similar: the major alkane products are ethane and butanes, and the minor products are methane and pentanes. These products are produced since a [2 + 2] cycloaddition of propene with W−alkylidenes would yield two different W−metallacyclobutanes as intermediates. The steric interactions between positions [1,2] and [1,3] of the substituents on the W−metal-

dx.doi.org/10.1021/ja410747g | J. Am. Chem. Soc. 2014, 136, 1054−1061

lacyclobutanes direct the alkene selectivity,[35] which upon hydrogenolysis yields the observed alkanes (see Scheme S1 in the Supporting Information).[35] The formation of branched alkanes results from the competitive σ bond activation of CH_2 versus CH_3 groups of the propane, which is well-documented in the literature.[4]

NMR Studies of the Thermal Transformation of 2. The above observations all suggest that the reaction proceeds through a W−methylidene intermediate. In order to induce the formation of this species, and in the hope of isolating the methylidene, we therefore studied the thermal stability of **2** in the absence of substrate directly by solid-state NMR.

Heating a supported sample of **2** which was enriched in ^{13}C (>95%) from 298 to 345 K leads to the observation of several new NMR signals. After maintaining the temperature at 345 K for 12 h, most of the ≡Si−O−W(Me)$_5$ had converted. The spectra of the converted material suggest that the products are the W−methyl/methylidyne species **5** and **6** in Scheme 3.

Scheme 3. Formation of the W−Methylidyne Species upon Heating 2

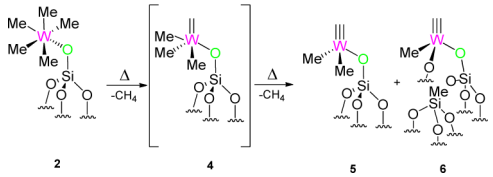

In the converted material the ^1H NMR spectrum (Figure 4) exhibits four major new signals at 1.1, 1.4, 4.1, and 7.6 ppm.

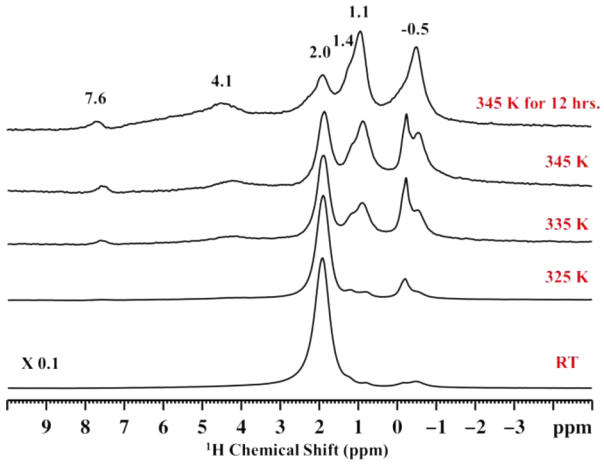

Figure 4. ^1H spin echo MAS solid-state NMR spectra of the thermal transformation of **2** (acquired on a 600 MHz NMR spectrometer with 20 kHz MAS frequency, number of scans 8, repetition delay 5 s). The true sample temperatures were calibrated by separately measuring the ^{79}Br isotropic chemical shifts and longitudinal relaxation times of KBr.[25]

The signals at 1.1, 1.4, and 4.1 ppm autocorrelate in 2D DQ and TQ $^1H-^1H$ homonuclear dipolar correlation spectra and are assigned to different methyl groups (Figure 5B,C). The proton resonance at 7.6 ppm displays no autocorrelation in the DQ and TQ spectra (Figure 5B,C). The broad signal at −0.5 ppm is assigned to methane and methyl groups transferred to silica (i.e., ≡SiMe), which is supported by an autocorrelation in DQ and TQ (Figure 5B,C) and also by ^{29}Si CP/MAS NMR

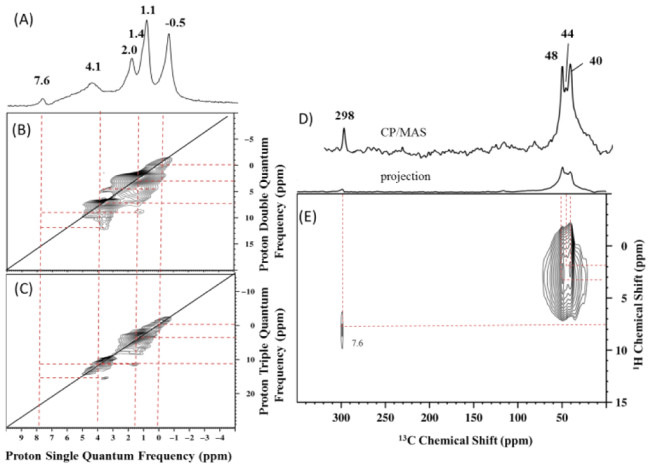

Figure 5. (A) 1D ^1H spin−echo MAS solid-state NMR spectrum of [(≡SiO)$_x$W(≡CH)Me$_y$] after maintaining the temperature of 95% ^{13}C -labeled **2** at 345 K for 12 h (acquired on a 600 MHz NMR spectrometer at a 20 kHz MAS spinning frequency, number of scans 8, repetition delay 5 s). (B) 2D $^1H-^1H$ DQ and (C) $^1H-^1H$ TQ (acquired on a 600 MHz NMR spectrometer at 22 kHz MAS spinning frequency with a back-to-back recoupling sequence, number of scans 128, repetition delay 5 s, number of t_1 increments 128, with the increment set equal to one rotor period of 45.45 μs) (D) ^{13}C CP/MAS NMR spectrum (10 kHz MAS at the same field as above, number of scans 20000, repetition delay 4 s, contact time 2 ms, line broadening 80 Hz). (E) 2D CP/MAS HETCOR NMR spectrum acquired with short contact times of 0.2 ms (8.5 kHz MAS, number of scans per increment 4000, repetition delay 4 s, number of t_1 increments 32, line broadening 80 Hz).

(peak at −12 ppm) (Figure S8, Supporting Information). The signal at 2.0 ppm likely corresponds to unreacted silanol. The ^{13}C CP/MAS NMR spectrum (Figure 5D) displays three signals at 40, 44, and 48 ppm, and at high frequency a signal at 298 ppm is observed. Additionally, the 2D $^1H-^{13}C$ HETCOR NMR spectrum (Figure 5E) with a short contact time (0.2 ms) shows a correlation between the methyl protons (1.4 and 1.1 ppm) and these two carbon atoms (44 and 40 ppm), respectively, and a correlation between the methyl protons centered at 4.1 ppm with the carbon at 48 ppm allows the assignment of the carbon−proton pairs to the individual methyl groups. Furthermore, the strong correlation between the carbon and proton signals at 298 and 7.6 ppm, respectively, strongly supports the assignment of a methylidyne moiety (W≡CH) (Figure 5E). Chemical shift values for ^1H and ^{13}C in this range are also reasonably consistent with DFT calculations for a model silica surface-supported system that contains a W≡CH functional group (see Figure S9 and Tables S5 and S6 in the Supporting Information).

Furthermore, a correlation in the DQ/SQ NMR correlation spectrum between the ≡SiCH$_3$ group at −0.5 ppm and the methyl groups at 4.1 ppm supports transfer of a methyl group to the silica and suggests the formation of bipodal species **6** (^{13}C, 48 ppm; ^1H, 4.1 ppm) (Scheme 3). Since no correlation with the other two methyl groups is observed, these two inequivalent methyl groups (^{13}C, 44 and 40 ppm; ^1H, 1.4 and 1.1 ppm) can be assigned to the monopodal species **5**. The methyl groups of both species **5** and **6** correlate with the methylidyne moiety as observed in both DQ and TQ NMR experiments (Figure 5B,C).

dx.doi.org/10.1021/ja410747g | J. Am. Chem. Soc. 2014, 136, 1054−1061

Backing for the Existence of Transient Methylidene Intermediates by Formation of W−Methyl/Methylidyne Species. Together, these studies suggest that **2** evolves upon thermal treatment into a mixture of unprecedented mono- and bipodal W−methyl/methylidyne species. This plausibly supports the formation of the transient W−methylidene intermediate **4** (Scheme 3). We have identified that the grafted WMe_6 species can evolve into a W−methylidyne-containing species, which would not be otherwise observable in a comparable homogeneous system.[36] These supported W−methylidyne species **5** and **6** were also used as precursors for propane metathesis and produced ethane and butane with traces of methane and pentanes with a TON of 50 after 120 h at 150 °C. We find that they are less active than the pentamethyl compound **2**. We very tentatively hypothesize that this is again due to the presence of fewer methyl groups. If we assume that the first step in the process was σ bond activation, it would then be easier for species **2** to achieve this, in comparison to species **5** or **6**.

■ CONCLUSION

We described the grafting of WMe_6 on variously dehydroxylated silica (at 200 and 700 °C) surfaces using surface organometallic strategies and tools. Notably, solid-state NMR combined with computational modeling offers significant support for the structure of a well-defined supported W species, $\equiv$Si−O−WMe_5, a surface species that is much more stable than the homoleptic parent complex in solution or in the solid state. Furthermore, the grafting of this unique WMe_6 homoleptic species allowed us to observe by solid state NMR the temperature dependence of the methyl ligand fluxionality at room temperature. Solid-state NMR has been used to qualitatively determine the podality (i.e., monopodal vs bipodal) of the grafted complex on silica. Then, thermal studies on $\equiv$Si−O−WMe_5 (**2**) led us to isolate a novel supported W−methylidyne/methyl complex, which was also confirmed by experimental and theoretical studies. All of these complexes are more active than the previously reported silica-supported W complexes in alkane metathesis, with a TON of 127 at 150 °C for $\equiv$Si−O−WMe_5.

■ EXPERIMENTAL SECTION

General Procedure. All experiments were carried out by using standard Schlenk and glovebox techniques under an inert nitrogen atmosphere. The syntheses and the treatments of the surface species were carried out using high-vacuum lines ($<10^{-5}$ mbar) and glovebox techniques. Pentane was distilled from a Na/K alloy under N_2 and dichloromethane from CaH_2. Both solvents were degassed through freeze−pump−thaw cycles. $SiO_{2\text{-}700}$ and $SiO_{2\text{-}200}$ were prepared from Aerosil silica from Degussa (specific area of 200 m^2/g), which were partly dehydroxylated at either 700 or 200 °C under high vacuum ($<10^{-5}$ mbar) for 24 h to give a white solid having a specific surface area of 190 m^2/g and containing respectively 0.5−0.7 and 2.4−2.6 OH/nm^2. Hydrogen and propane were dried and deoxygenated before use by passage through a mixture of freshly regenerated molecular sieves (3 Å) and R$\bar{3}$-15 catalysts (BASF). IR spectra were recorded on a Nicolet 6700 FT-IR spectrometer by using a DRIFT cell equipped with CaF_2 windows. The IR samples were prepared under argon within a glovebox. Typically, 64 scans were accumulated for each spectrum (resolution 4 cm^{-1}). Elemental analyses were performed at Mikroanalytisches Labor Pascher (Germany). Gas-phase analysis of alkanes was performed using an Agilent 6850 gas chromatography column with a split injector coupled with an FID (flame ionization detector). An HP-PLOT Al_2O_3 KCl 30 m × 0.53 mm, 20.00 mm capillary column coated with a stationary phase of aluminum oxide deactivated with KCl was used with helium as the carrier gas at 32.1 kPa. Each analysis was carried out under the same conditions: a flow rate of 1.5 mL/min and an isotherm at 80 °C.

Liquid-State Nuclear Magnetic Resonance Spectroscopy. All liquid-state NMR spectra were recorded on Bruker Avance 600 MHz spectrometers. All chemical shifts were measured relative to the residual ^1H or ^{13}C resonance in the deuteurated solvent: CD_2Cl_2, 5.32 ppm for ^1H, 53.5 ppm for ^{13}C.

Solid-State Nuclear Magnetic Resonance Spectroscopy. One-dimensional ^1H MAS and ^{13}C CP/MAS solid state NMR spectra were recorded on Bruker AVANCE III spectrometers operating at 400, 500, or 700 MHz resonance frequencies for ^1H. ^{29}Si NMR solid-state NMR was recorded using a 400 MHz Bruker AVANCE III spectrometer. Experiments at 400 MHz employed a conventional double-resonance 4 mm CP/MAS probe, while experiments at 700 MHz utilized a 3.2 mm HCN triple-resonance probe. For the 150 K experiment on **3** at 400 MHz, a Bruker low-temperature 3.2 mm double-resonance probe was employed. In all cases the samples were packed into rotors under an inert atmosphere inside gloveboxes. Dry nitrogen gas was utilized for sample spinning to prevent degradation of the samples. NMR chemical shifts are reported with respect to the external references TMS and adamantane. For ^{13}C and ^{29}Si CP/MAS NMR experiments, the following sequence was used: 90° pulse on the proton (pulse length 2.4 s), then a cross-polarization step with a contact time of typically 2 ms, and finally acquisition of the ^{13}C and ^{29}Si NMR signal under high-power proton decoupling. The delay between the scans was set to 5 s to allow the complete relaxation of the ^1H nuclei, and the number of scans ranged between 3000 and 5000 for ^{13}C and 30000 and 50000 for ^{29}Si and was 32 for ^1H. An exponential apodization function corresponding to a line broadening of 80 Hz was applied prior to Fourier transformation.

The 2D $^1H-^{13}C$ heteronuclear correlation (HETCOR) solid state NMR spectroscopy experiments were conducted on a Bruker AVANCE III spectrometer using a 3.2 mm MAS probe. The experiments were performed according to the following scheme: 90° proton pulse, t_1 evolution period, CP to ^{13}C, and detection of the ^{13}C magnetization under TPPM decoupling. For the cross-polarization step, a ramped radio frequency (RF) field centered at 75 kHz was applied to the protons, while the ^{13}C channel RF field was matched to obtain an optimal signal. A total of 32 t_1 increments with 2000 scans each were collected. The sample spinning frequency was 8.5 kHz. Using a short contact time (0.5 ms) for the CP step, the polarization transfer in the dipolar correlation experiment was verified to be selective for the first coordination sphere about the tungsten: that is, to lead to correlations only between pairs of attached $^1H-^{13}C$ spins (C−H directly bonded).

$^1H-^1H$ Multiple-Quantum Spectroscopy. Two-dimensional double-quantum (DQ) and triple-quantum (TQ) experiments were recorded on a Bruker AVANCE III spectrometer operating at 600 MHz with a conventional double-resonance 3.2 mm CP/MAS probe, according to the following general scheme: excitation of DQ coherences, t_1 evolution, z filter, and detection. The spectra were recorded in a rotor synchronized fashion in t_1 by setting the t_1 increment equal to one rotor period (45.45 μs). One cycle of the standard back-to-back (BABA) recoupling sequences was used for the excitation and reconversion period.[37] Quadrature detection in w_1 was achieved using the States-TPPI method. An MAS frequency of 22 kHz was used. The 90° proton pulse length was 2.5 μs, while a recycle delay of 5 s was used. A total of 128 t_1 increments with 32 scans per each increment were recorded. The DQ frequency in the w_1 dimension corresponds to the sum of two single-quantum (SQ) frequencies of the two coupled protons and correlates in the w_2 dimension with the two corresponding proton resonances.[38] The TQ frequency in the w_1 dimension corresponds to the sum of the three SQ frequencies of the three coupled protons and correlates in the w_2 dimension with the three individual proton resonances. Conversely, groups of less than three equivalent spins will not give rise to diagonal signals in this spectrum.

Preparation of Hexamethyltungsten, WMe_6 (1). The molecular precursor WMe_6 (**1**) was prepared from WCl_6 and $(CH_3)_2Zn$,

dx.doi.org/10.1021/ja410747g | J. Am. Chem. Soc. 2014, 136, 1054−1061

following the literature procedure.[12,19,39] To a mixture of WCl_6 (1.80 g, 4.5 mmol) in dichloromethane (25 mL) was added $(CH_3)_2Zn$ (13.6 mmol, 1.0 M in heptane) at −80 °C, and after addition, the reaction mixture was warmed to −35 °C and stirred at this temperature for another 30 min. After successive filtrations with pentane and removal of the solvent, the red solid **1** was obtained (0.16 g, 12%). *Caution!* This 12e compound is highly unstable and is prone to violent decomposition.[40] ^{1}H NMR (CD_2Cl_2, 600 MHz): δ (ppm) 1.65 (s, 18H, WCH_3). ^{13}C NMR (CD_2Cl_2, 150 MHz): δ (ppm) 82 (s, 6C, $J^{183}_{W-^{13}C}$ = 47 Hz, WCH_3). HSQC confirms the correlation between the ^{1}H and ^{13}C NMR signals.

The ^{13}C-enriched $W(CH_3)_6$ was synthesized as described below: ^{13}C-enriched $(^{13}CH_3)_2Zn$ was prepared from a suspension of $^{13}CH_3Li$ and $ZnCl_2$ (2/1), with subsequent synthetic steps being analogous to those provided above.[41]

Preparation of WMe_6 on $SiO_{2\text{-}700}$ (2). A solution of **1** in pentane (150 mg, 1.2 equiv with respect to the amount of surface-accessible silanols) was reacted with 1.8 g of Aerosil $SiO_{2\text{-}700}$ at −50 °C for 1 h, was warmed to −30 °C, and was stirred for an additional 2 h. At the end of the reaction, the resulting yellow solid was washed with pentane (3 × 20 mL) and dried under dynamic vacuum (<10^{-5} Torr, 1 h). IR data (cm^{-1}): 3742, 3014, 2981, 2946, 2878, 1410. ^{1}H solid-state NMR (400 MHz): δ (ppm) 2.0 (W−CH_3). ^{13}C CP/MAS solid-state NMR (100 MHz): δ (ppm) 82.0 (W−CH_3). Anal. Found: W, 3.5−3.9; C, 1.1−1.3. The C/W ratio obtained was 5.0 ± 0.1 (5 was expected).

Preparation of 3. The same procedure above was carried out with Aerosil $SiO_{2\text{-}200}$ dehydroxylated at 200 °C. ^{1}H solid-state NMR (400 MHz): δ (ppm) 1.95 (W−CH_3). ^{13}C CP/MAS solid-state NMR (100 MHz): δ (ppm) 80.4 (W−CH_3). Anal. Found: W, 3.49; C, 1.04. The C/W ratio obtained was 4.6 ± 0.1 (4.7 was expected).

Synthesis of 5 and 6. In a glass reactor, 1.25 g of **2** was added and heated at 100 °C (ramped at 60 °C/h) for 12 h to produce a dark gray powder which was a mixture of the monopodal and bipodal species **5** and **6**. IR data (cm^{-1}): 3741, 2967, 2929, 2899. ^{1}H solid-state NMR (400 MHz): δ (ppm) −0.5 (s, Si−CH_3), 1.1 (s, W−CH_3), 1.4 (s, W−CH_3), 2.0 (s, SiOH), 4.1 (s, W−CH_3), 7.6 (s, W≡CH). ^{13}C CP/MAS solid-state NMR (100 MHz): δ (ppm) 40 (s, W−CH_3), 44 (s, W−CH_3), 48 (s, W−CH_3), 298 (s, W≡CH). ^{29}Si CP/MAS solid-state NMR (80 MHz): δ (ppm) −12.3 (≡SiCH$_3$), −100 (Q3), −109.7 (Q4). Anal. Found: W, 3.18; C, 0.6. The C/W ratio obtained was 2.9 ±0.1 (3 was expected).

Procedure for the Quantification of Methane Released during Hydrogenolysis. A sample of **2** (0.020 mmol/W, 100 mg) and dry H_2 (786 hPa) was added in a batch reactor of known volume (480 mL). The reaction mixture was heated to 130 °C for 10 h. Next, an aliquot of the gas phase was released and analyzed by GC. Gas-phase analysis gave 0.098 mmol of CH_4, corresponding to a C/W ratio of 4.9 ± 0.1 (5 was expected).

Typical Procedure for Propane Metathesis Reactions. A mixture of a potential catalytic material (0.013 mmol/W) and dry propane (980−1013 hPa) were heated to 150 °C in a batch reactor of known volume (480 mL) over a 5 day period. At the end of the run, an aliquot was drawn and analyzed by GC. The selectivities are defined as the amount of a particular product molecule over the total amount of products.

Computational Details. All quantum chemical computations were performed using the Amsterdam Density Functional (ADF) software, version 2010.02,[42,43] which is produced by Scientific Computing & Modeling (SCM). For both the geometry optimization and the magnetic shielding calculations (^{1}H and ^{13}C), the zeroth-order regular approximation (ZORA)[44−46] was used to include relativistic effects and included both scalar and spin−orbit contributions.[47] All calculations used an all-electron triple-ζ basis set which included polarization functions (i.e., TZ2P) and the generalized gradient approximation (GGA) exchange-correlation functional developed by Perdew, Burke, and Ernzerhof (i.e., PBE).[48,49] Magnetic shielding calculations were carried out using the "NMR" module which comes bundled with the ADF software.

For models of monopodal species on $SiO_{2\text{-}700}$, the silica surface selected for NMR property computations was taken from the previously optimized structure of Emsley and co-workers.[22] The surface species was exchanged from that of the prior study with the species of interest here, and the surface was truncated at the second coordination sphere for the magnetic shielding tensor computation. Where applicable, oxygen atoms from the silica surface were terminated with hydrogen atoms. For all monopodal surfaces, the silicon and oxygen atoms of the surface were fully frozen, while the surface species of interest, as well as the H atoms terminating the silica surface, were fully optimized at the level of theory specified earlier. Optimized geometries and energies, as well as a more complete disclosure of the computed magnetic shielding values, are provided in the Supporting Information.

For models of bipodal species on $SiO_{2\text{-}200}$, the silica surface was taken from Sautet and co-workers.[50] The surface corresponds to a slice along the [001] plane of β-cristobalite and was found to be a stable phase of silica under the approximate conditions of the material under study (i.e., 200 °C and near-ambient pressures). Taking the original structure proposed by the authors (denoted as **001-4** in the original manuscript), a small cluster was selected and terminated with hydrogen atoms at all but two central positions. For these two positions, the surface species was placed. All framework atoms, except for the directly bound oxygen atoms, were held fixed, while the molecule on the surface was subjected to a geometry optimization.

In comparison to the monopodal species, many computational parameters remained identical (i.e., basis set, exchange-correlation functional, ZORA), but they were supplemented by a dispersion term (given by Grimme's three-parameter description)[51] due to the large size of the cluster. The additional dispersion correction leads to a slightly more favorable interaction between the molecule and the surface. As before, optimized geometries and energies, as well as a more complete disclosure of the computed magnetic shielding values, are provided in the Supporting Information.

■ ASSOCIATED CONTENT

Supporting Information

Figures and tables giving solution NMR spectra of **1**, additional solid-state NMR spectra of **2** and **3**, variable-temperature ^{1}H, ^{13}C, and ^{29}Si solid-state NMR spectra of **3**, and information on optimized geometries and full disclosure of the calculated magnetic shielding values for the computational models used. This material is available free of charge via the Internet at http://pubs.acs.org.

■ AUTHOR INFORMATION

Corresponding Author

jeanmarie.basset@kaust.edu.sa (J.-M.B.); emmanuel.callens@kaust.edu.sa (E.C.).

Notes

The authors declare no competing financial interest.

■ ACKNOWLEDGMENTS

The authors acknowledge the KAUST Nuclear Magnetic Resonance Core Lab and technical assistance of Dr. Kazuo Yamauchi. The authors also thank Dr. Nassima Riache for her fruitful discussions. Mr. Benoît Vincenti is thanked for inert-atmosphere sample preparation prior to solid-state NMR experiments upon **2**. A.J.R. acknowledges support from an EU Marie-Curie IIF fellowship (PIIF-GA-2010-274574). C.M.W. acknowledges the Natural Sciences and Engineering Council of Canada (NSERC) for a postdoctoral fellowship. Computational resources for DFT calculations were provided by the Pôle Scientifique de Modélisation Numérique (PSMN). This work was supported by funds from King Abdullah University of Science and Technology.

REFERENCES

(1) Basset, J. M.; Copéret, C.; Soulivong, D.; Taoufik, M.; Thivolle-Cazat, J. *Angew. Chem., Int. Ed.* **2006**, *45*, 6082−6085.
(2) Burnett, R. L.; Hughes, T. R. *J. Catal.* **1973**, *31*, 55−64.
(3) Haibach, M. C.; Kundu, S.; Brookhart, M.; Goldman, A. S. *Acc. Chem. Res.* **2012**, *45*, 947−958.
(4) Basset, J. M.; Copéret, C.; Soulivong, D.; Taoufik, M.; Cazat, J. T. *Acc. Chem. Res.* **2010**, *43*, 323−334.
(5) Vidal, V.; Theolier, A.; Thivolle-Cazat, J.; Basset, J. M. *Science* **1997**, *276*, 99−102.
(6) Le Roux, E.; Taoufik, M.; Copéret, C.; de Mallmann, A.; Thivolle-Cazat, J.; Basset, J. M.; Maunders, B. M.; Sunley, G. J. *Angew. Chem., Int. Ed.* **2005**, *44*, 6755−6758.
(7) Taoufik, M.; Le Roux, E.; Thivolle-Cazat, J.; Copéret, C.; Basset, J. M.; Maunders, B.; Sunley, G. J. *Top. Catal.* **2006**, *40*, 65−70.
(8) Rascon, F.; Copéret, C. *J. Organomet. Chem.* **2011**, *696*, 4121−4131.
(9) Chauvin, Y. *Angew. Chem., Int. Ed.* **2006**, *45*, 3740−3747.
(10) Copéret, C. *Chem. Rev.* **2010**, *110*, 656−680.
(11) Blanc, F.; Berthoud, R.; Copéret, C.; Lesage, A.; Emsley, L.; Singh, R.; Kreickmann, T.; Schrock, R. R. *Proc. Natl. Acad. Sci. U.S.A.* **2008**, *105*, 12123−12127.
(12) Shortland, A. J.; Wilkinson, G. *J. Chem. Soc., Chem. Commun.* **1972**, 318.
(13) Schrock, R. R. *J. Am. Chem. Soc.* **1974**, *96*, 6796−6797.
(14) Buffon, R.; Leconte, M.; Choplin, A.; Basset, J. M. *J. Chem. Soc., Dalton Trans.* **1994**, 1723−1729.
(15) Le Roux, E.; Taoufik, M.; Chabanas, M.; Alcor, D.; Baudouin, A.; Copéret, C.; Thivolle-Cazat, J.; Basset, J. M.; Lesage, A.; Hediger, S.; Emsley, L. *Organometallics* **2005**, *24*, 4274−4279.
(16) Smith, J.; Mowat, W.; Whan, D. A.; Ebsworth, E. A. V. *J. Chem. Soc., Dalton Trans.* **1974**, 1742−1746.
(17) Mowat, W.; Smith, J.; Whan, D. A. *J. Chem. Soc., Chem. Commun.* **1974**, 34−35.
(18) Copéret, C.; Chabanas, M.; Saint-Arroman, R. P.; Basset, J. M. *Angew. Chem., Int. Edit.* **2003**, *42*, 156−181.
(19) Kleinhenz, S.; Pfennig, V.; Seppelt, K. *Chem. Eur. J.* **1998**, *4*, 1687−1691.
(20) Geen, H.; Titman, J. J.; Gottwald, J.; Spiess, H. W. *Chem. Phys. Lett.* **1994**, *227*, 79−86.
(21) Fleischman, S. D.; Scott, S. L. *J. Am. Chem. Soc.* **2011**, *133*, 4847−4855.
(22) Blanc, F.; Basset, J. M.; Copéret, C.; Sinha, A.; Tonzetich, Z. J.; Schrock, R. R.; Solans-Monfort, X.; Clot, E.; Eisenstein, O.; Lesage, A.; Emsley, L. *J. Am. Chem. Soc.* **2008**, *130*, 5886−5900.
(23) Chen, Y.; Callens, E.; Abou-Hamad, E.; Merle, N.; White, A. J. P.; Taoufik, M.; Copéret, C.; Le Roux, E.; Basset, J. M. *Angew. Chem., Int. Ed.* **2012**, *51*, 11886−11889.
(24) Elena, B.; de Paepe, G.; Emsley, L. *Chem. Phys. Lett.* **2004**, *398*, 532−538.
(25) Thurber, K. R.; Tycko, R. *J. Magn. Reson.* **2009**, *196*, 84−87.
(26) Landis, C. R.; Cleveland, T.; Firman, T. K. *J. Am. Chem. Soc.* **1995**, *117*, 1859−1860.
(27) Landis, C. R.; Cleveland, T.; Firman, T. K. *Science* **1996**, *272*, 182.
(28) (a) Demolliens, A.; Jean, Y.; Eisenstein, O. *Organometallics* **1986**, *5*, 1457−1464. (b) Kang, S. K.; Albright, T. A.; Eisenstein, O. *Inorg. Chem.* **1989**, *28*, 1611−1613.
(29) Freudenberger, J. H.; Schrock, R. R. *Organometallics* **1985**, *4*, 1937−1944.
(30) Kreickmann, T.; Arndt, S.; Schrock, R. R.; Muller, P. *Organometallics* **2007**, *26*, 5702−5711.
(31) Pfennig, V.; Seppelt, K. *Science* **1996**, *271*, 626−628.
(32) Gajan, D.; Copéret, C. *New J. Chem.* **2011**, *35*, 2403−2408.
(33) It is important to point out here that it is difficult to compare the calculated magnetic shielding values for the monopodal and bipodal structural models on an absolute basis, as the surfaces used in the models are very different. With this being said, the differences (i.e., using a relative basis) between the magnetic shielding values offer a much better platform on which to compare and contrast the two structures. For example, the range of the carbon chemical shifts for the bipodal species is reduced relative to the monopodal species, and in addition the bipodal species would possess carbon chemical shifts which are generally larger than those for the monopodal species.
(34) Le Roux, E.; Taoufik, M.; Baudouin, A.; Copéret, C.; Thivolle-Cazat, J.; Basset, J. M.; Maunders, B. M.; Sunley, G. J. *Adv. Synth. Catal.* **2007**, *349*, 231−237.
(35) (a) Le Roux, E.; Chabanas, M.; Baudouin, A.; de Mallmann, A.; Copéret, C.; Quadrelli, E. A.; Thivolle-Cazat, J.; Basset, J. M.; Lukens, W.; Lesage, A.; Emsley, L.; Sunley, G. J. *J. Am. Chem. Soc.* **2004**, *126*, 13391−13399. (b) Leconte, M.; Basset, J. M. *J. Am. Chem. Soc.* **1979**, *101*, 7296−7302.
(36) Chiu, K. W.; Jones, R. A.; Wilkinson, G.; Galas, A. M. R.; Hursthouse, M. B.; Malik, K. M. A. *J. Chem. Soc., Dalton Trans.* **1981**, 1204−1211.
(37) Sommer, W.; Gottwald, J.; Demco, D. E.; Spiess, H. W. *J. Magn. Reson.* **1995**, *113*, 131−134.
(38) Rataboul, F.; Baudouin, A.; Thieuleux, C.; Veyre, L.; Copéret, C.; Thivolle-Cazat, J.; Basset, J. M.; Lesage, A.; Emsley, L. *J. Am. Chem. Soc.* **2004**, *126*, 12541−12550.
(39) Shortland, A. J.; Wilkinson, G. *J. Chem. Soc., Dalton Trans.* **1973**, 872−876.
(40) Seppelt, K. *Science* **1996**, *272*, 182−183.
(41) DuMez, D. D.; Mayer, J. M. *J. Am. Chem. Soc.* **1996**, *118*, 12416−12423.
(42) te Velde, G.; Bickelhaupt, F. M.; Baerends, E. J.; Guerra, C. F.; van Gisbergen, S. J. A.; Snijders, J. G.; Ziegler, T. *J. Comput. Chem.* **2001**, *22*, 931−967.
(43) Guerra, C. F.; Snijders, J. G.; te Velde, G.; Baerends, E. J. *Theor. Chem. Acc.* **1998**, *99*, 391−403.
(44) van Lenthe, E.; Ehlers, A.; Baerends, E. J. *J. Chem. Phys.* **1999**, *110*, 8943−8953.
(45) van Leeuwen, R.; Baerends, E. J. *Int. J. Quantum Chem.* **1994**, *52*, 711−730.
(46) van Lenthe, E.; Baerends, E. J.; Snijders, J. G. *J. Chem. Phys.* **1993**, *99*, 4597−4610.
(47) van Lenthe, E.; Snijders, J. G.; Baerends, E. J. *J. Chem. Phys.* **1996**, *105*, 6505−6516.
(48) Perdew, J. P.; Burke, K.; Ernzerhof, M. *Phys. Rev. Lett.* **1997**, *78*, 1396.
(49) Perdew, J. P.; Burke, K.; Ernzerhof, M. *Phys. Rev. Lett.* **1996**, *77*, 3865−3868.
(50) Rozanska, X.; Delbecq, F.; Sautet, P. *Phys. Chem. Chem. Phys.* **2010**, *12*, 14930−14940.
(51) Grimme, S.; Antony, J.; Ehrlich, S.; Krieg, H. *J. Chem. Phys.* **2010**, *132*, 154104−154123.